Case Report | Neuroimaging and Head and Neck

http://dx.doi.org/10.3348/kjr.2014.15.1.156
pISSN 1229-6929 · eISSN 2005-8330
Korean J Radiol 2014;15(1):156-160

Korean Journal of Radiology
KJR

Hyperostotic Esthesioneuroblastoma: Rare Variant and Fibrous Dysplasia Mimicker

Manzoor Ahmed, MD[1], Phillip Daniel Knott, MD[2]

[1]Neuroradiology Section, Imaging Institute, Cleveland Clinic Foundation, Cleveland, OH 44195, USA; [2]Director of Facial Plastic and Reconstructive Surgery, Associate Professor of Otolaryngology, UCSF School of Medicine, San Fransisco, CA 94143, USA

A 65-year-old male presented with a 3-year history of orbital symptoms. An imaging-based diagnosis of fibrous dysplasia involving the skull base was made at another institution. CT showed a diffuse sinonasal mass and ground-glass appearance of the bones of the anterior skull base with bony defects and mucocele formation. MRI demonstrated an accompanying intracranial and orbital rind of soft tissue mass along the hyperostotic bones. FDG-PET showed corresponding intense hypermetabolism. Small cysts were observed at the tumor-brain interface. Biopsy revealed esthesioneuroblastoma with bone infiltration that is compatible with the hyperostotic variant of esthesioneuroblastoma. There are a few cases of hyperostotic esthesioneuroblastoma reported in the literature.

Index terms: *Fibrous dysplasia; Esthesioneuroblastoma; Hyperostosis*

INTRODUCTION

A wide variety of benign and malignant tumors can originate in the sinonasal region, including hamartomas (1, 2). Esthesioneuroblastoma (ENB) or olfactory neuroblastoma (ONB) is an uncommon type of neuroectodermal tumor that is specific to the sinonasal tract (3). It accounts for about 3-6% of all intranasal tumours (4, 5). ENB is derived from the specialized olfactory epithelium, which lines the superior portion of the nasal cavity. The origin of ENB is generally confined to the distribution of olfactory epithelium, specifically the cribriform plate, the superior turbinate, and the superior one-third of the nasal septum (6). As a result of its origin in the superior nasal cavity, the tumor typically invades the superomedial orbit and the anterior cranial fossa; the tumor invades the latter through the cribriform plate of the ethmoid bone. Bone invasion by any malignant sinonasal tumor is via osteolysis and is observed as a lytic pattern on CT imaging. Rarely, the osteoblasts are involved in bone invasion resulting in exuberant bone formation. In the English literature, we found only four cases of hyperostotic ENB causing bone invasion (7, 8). Regenbogen et al. (7) first used the term, “hyperostotic" ENB. In our case, bone infiltration and dominant hyperostosis, mimicking fibrous dysplasia were depicted on three imaging modalities. The indolent course of hyperostotic ENB may be potentially related to this predominant pattern of bone infiltration. However, the indolent course of hyperostotic ENB cannot be clearly determined due to the limited number of reported cases in the literature.

Received March 7, 2013; accepted after revision October 27, 2013.
Corresponding author: Manzoor Ahmed, MD, Neuroradiology Section, Imaging Institute, Cleveland Clinic Foundation, Ohio 9500, Euclid Avenue, Cleveland, OH 44195, USA.
• Tel: (1216) 444 1084 • Fax: (1216) 201 5124
• E-mail: sohakhan022006@yahoo.com

Korean Journal of Radiology
KJR

CASE REPORT

A 65-year-old male initially presented at another institution with mild visual disturbances, loss of taste, and proptosis. CT imaging was suggestive of fibrous dysplasia. No treatment was administered at that time. Serial imaging performed over three years showed slow progression of the lesion? with no significant clinical deterioration. The patient was subsequently referred to our institution. CT, MRI and FDG-PET imaging were performed. CT (Fig. 1A, B) showed expansile, diffuse hyperostosis of the ethmoid bones, nasal septum, superomedial orbital walls and anterior frontal skull base. There was an extensive intracranial and extracranial enhancing soft tissue thickening along the hyperostotic bones. MRI (Fig. 1C, D) showed hypointense T1 and T2 signals of the bone marrow that corresponded to the hyperostotic bones on CT, with moderate diffuse enhancement. The rind of soft tissue mass along the hyperostotic bones showed hypointense to isointense T1 and T2 signals and diffuse enhancement. Intracranial rim enhancing small cysts were observed at the tumor-brain interface. Multi-focal extracranial mucoceles were also identified. FDG-PET (Fig. 1E, F) showed a corresponding diffuse hypermetabolic uptake in the soft tissues and bones. Endoscopic biopsies of the mass and bone confirmed the diagnosis of ONB with osseous tumor infiltration (Fig. 1G, H). The patient opted for non-surgical treatment and expired in about 2 years.

DISCUSSION

The typical imaging features of ENB have been

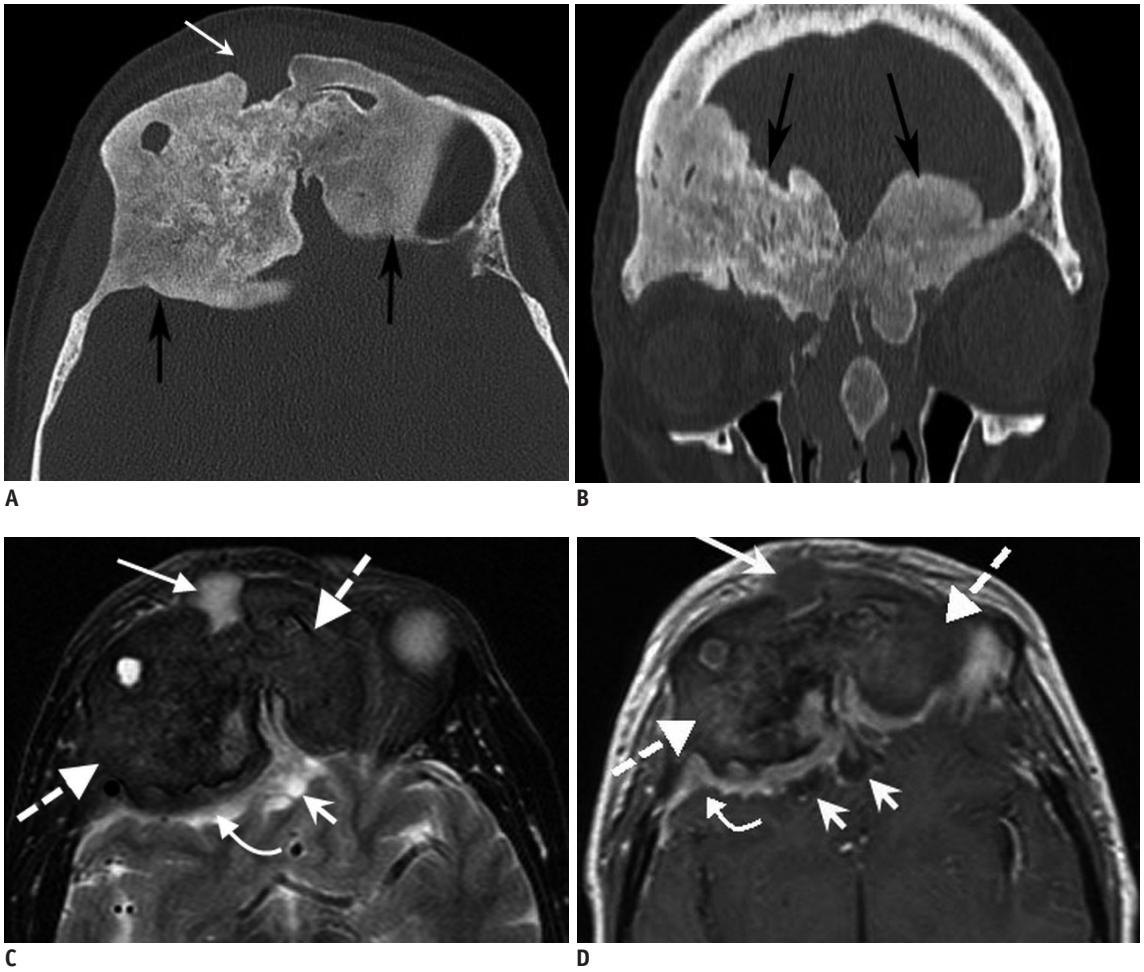

Fig. 1. Hyperostotic esthesioneuroblastoma in 65-year-old male mimicking fibrous dysplasia.
A, B. Axial and coronal CT images show diffuse sclerotic expansile bones of anterior skull base and superior sinonasal cavity (arrows). Hyperostotic bones show homogeneous, ground glass appearance. **C, D.** Axial T2 and post-contrast T1 fat saturated MR images show enhancing rind of soft tissue mass (curved arrows) along hyperostotic bones (dashed arrows) which shows mild heterogeneous enhancement. Note formation of small cysts at tumor-brain interface (short arrows). Note formation of mucocele (long arrow).

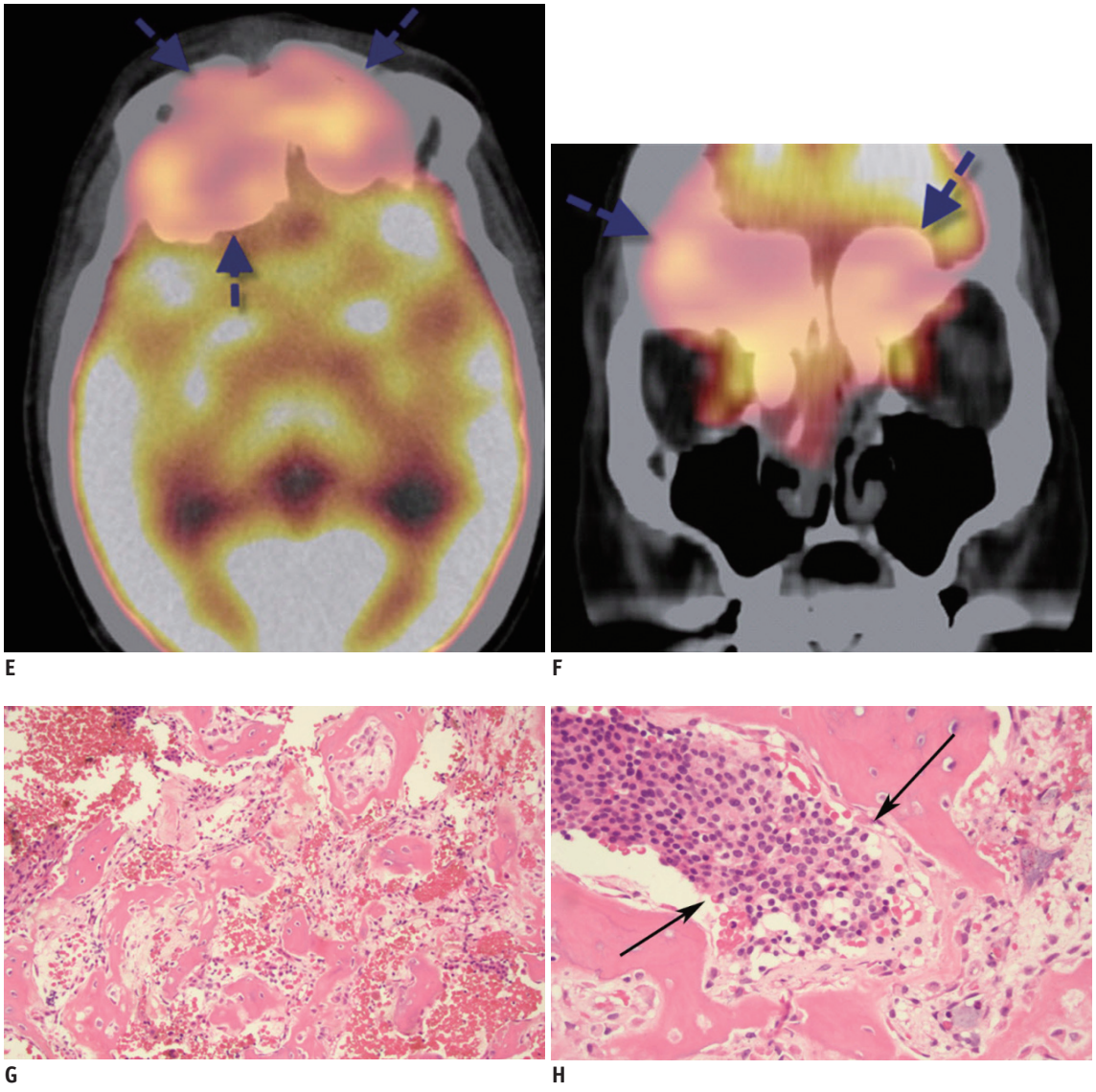

Fig. 1. Hyperostotic esthesioneuroblastoma in 65-year-old male mimicking fibrous dysplasia.
E, F. Axial and coronal FDG-PET CT fused color images show intense FDG avidity in hyperostotic bones (blue arrows) indicating diffuse tumor infiltration. Uptake in thin rind of soft tissue mass could not be separately visualized. **G, H.** Histologic images (H&E stains with 200 x **(G)** and 400 x **(H)** magnification). **(G)** Shows predominantly reactive bone formation, and **(H)** demonstrates sheet of tumor cells (arrows) within reactive bone.

described previously (9-11). CT usually shows an isodense to hyperdense expansile enhancing soft tissue mass with osteolytic bone erosion, and a speckled pattern of calcification within the tumor matrix is rarely observed. Occasionally, small foci of calcification may be seen (12, 13). MRI also shows non-specific features, the mass typically shows homogeneous enhancement, and hypointense to isointense signal on T1- and isointense to hyperintense signal on T2-weighted images (9). The heterogeneous appearance is due to cystic degeneration, necrosis and hemorrhagic foci. The presence of well-defined cysts at the tumor-brain interface is a relatively specific diagnostic indicator of ENB (14, 15). The soft tissue mass in the coronal plane of cross-sectional imaging can show the following features: 1) localization in the superior nasal cavity and ethmoid labyrinth, 2) limited erosion of the cribriform plate and/or medial/superior wall of the orbits, and 3) a large bulky extension into the anterior cranial fossa and/or orbits. The Kadish staging system divides tumors into 3 groups: group A lesions are limited to the nasal cavity; group B lesions involve the nasal cavity and paranasal sinuses; and group C lesions extend beyond the nasal cavity and paranasal sinuses. On the other hand, TNM staging provides more detailed information on the invasion

Korean Journal of Radiology
KJR

of the thats sound correct skull base and orbits (16).

Our case was classified as Kadish stage C. There was diffuse sinonasal, orbital, and frontal skull base hyperostosis and a diffuse rind of soft tissue mass along the margins of the hyperostotic bone. Typically, an ENB is observed as an osteolytic bony defect in the anterior skull base, which provides an easy conduit for bulky intracranial extension. Our case was a variant of ENB, and hence a large lytic bone defect was not observed and hyperostosis was the predominant finding. The hyperostotic ENB had a homogeneous ground-glass appearance, truly mimicking fibrous dysplasia. The mucocele formation indicated the chronicity of the process with obstructive sequelae and chronic rhinosinusitis. As expected, the hyperostotic tumor was hypointense on T1- and T2-weighted images. Diffuse enhancement of the involved bones indicated tumor infiltration. Diffuse hypermetabolism in the bone-soft tissue tumor complex on FDG-PET imaging corresponded to the biopsy-proven tumor in the hyperostotic bones and surrounding soft tissue. According to our experience as well as that described in the previous reports, large, bulky intracranial tumors are characterized by the presence of cysts at the tumor-brain interface. However, in this case, the cysts were present despite a smaller tumor bulk (i.e., sub-centimeter intracranial soft tissue thickening).

The previous three reported cases were of females while our patient was a male. The case reported by Schiro et al. (17) had a long clinical history of about seven years. Our case also had a long indolent course of about three years. The chronicity is manifested by secondary obstructive and mucosal stigmata in the sinuses. The current case had more extensive hyperostosis. FDG-PET findings of hyperostotic ENB have not been described previously, but FDG-PET may provide excellent details for tumor mapping.

The following are different potential causes of hyperostosis associated with tumors: hypervascularity, non-invasive irritation of the bone, hormone-mediated osteoblast stimulation, bone formation by the tumor, and most importantly, direct tumor invasion. Hyperostosis adjacent to skull-base meningiomas particularly sphenoid and peri-clinoid meningiomas ("hyperostotic meningiomas") is generally considered as a marker of bone invasion and necessitates surgical intervention (18). Hyperostosis associated with meningiomas is usually localized and proportional to the size of the tumor. However, the rare variant of ENB that was observed in our case showed more extensive hyperostosis.

This case report describes a rare variant of ENB, which truly mimics anterior skull base and sinonasal fibrous dysplasia. Ground-glass appearance of the bone matrix is a characteristic feature of fibrous dysplasia. Tehranzadeh et al. (19) compared fibrous dysplasia with Paget's disease of the skull using CT imaging. Ground-glass appearance, absence of cortical thickening, involvement of the paranasal sinuses and asymmetric findings were the specific features of fibrous dysplasia. The other less specific features which still favored the diagnosis of fibrous dysplasia included the following: orbital, nasal cavity, sphenoid or maxillary sinus involvement, soft tissue thickening, and cystic lucency of the hyperostotic bones. More symmetric bone involvement and cortical thickening were observed in Paget's disease, but ground-glass appearance, sino-nasal involvement, cystic lucencies or soft tissue thickening were not seen in Paget's disease. Only 3 cases of fibrous dysplasia showed soft tissue attenuation, which were proved to be fibrous stroma on histological examination. Chronic sinusitis can result in localized or diffuse sinonasal hyperostosis. The specific features of chronic sinusitis include retracted margins, sinus opacification, irregular hyperostosis and post-operative changes.

Like in our case, it may be very difficult to differentiate fibrous dysplasia from hyperostotic ENB on imaging. The latter condition can show most of the imaging features of fibrous dysplasia especially on CT. Enhancing soft tissue thickening along the hyperostotic bones and cysts at the tumor-brain interface are highly suggestive of hyperostotic ENB. FDG-PET was helpful for detecting the presence of the tumor as well as for mapping the extent of tumor in the bones.

Summary

Esthesioneuroblastoma typically results in osteolysis of the anterior skull base and or causes some degree of bone remodelling. Hyperostosis associated with bone invasion is a rare feature. In agreement with the existing literature on this disease, our case demonstrated ground-glass appearance and hyperostosis, mimicking fibrous dysplasia on CT. Unlike large bulky intracranial extension of the tumor, our case showed a diffuse rind of soft tissue mass along the hyperostotic tumor. FDG-PET can be used for tumor mapping in the hyperostotic bones. The abnormal bone on imaging proved to be a reactive bone as well as bony invasion by the tumor. Direct bone invasion is one of the many possible causes of hyperostosis as is evident from

the literature on skull base meningiomas.

REFERENCES

1. Eggesbø HB. Imaging of sinonasal tumours. *Cancer Imaging* 2012;12:136-152
2. Kim JE, Kim HJ, Kim JH, Ko YH, Chung SK. Nasal chondromesenchymal hamartoma: CT and MR imaging findings. *Korean J Radiol* 2009;10:416-419
3. Mills SE. Neuroectodermal neoplasms of the head and neck with emphasis on neuroendocrine carcinomas. *Mod Pathol* 2002;15:264-278
4. Svane-Knudsen V, Jørgensen KE, Hansen O, Lindgren A, Marker P. Cancer of the nasal cavity and paranasal sinuses: a series of 115 patients. *Rhinology* 1998;36:12-14
5. Broich G, Pagliari A, Ottaviani F. Esthesioneuroblastoma: a general review of the cases published since the discovery of the tumour in 1924. *Anticancer Res* 1997;17:2683-2706
6. Iezzoni JC, Mills SE. "Undifferentiated" small round cell tumors of the sinonasal tract: differential diagnosis update. *Am J Clin Pathol* 2005;124 Suppl:S110-S121
7. Regenbogen VS, Zinreich SJ, Kim KS, Kuhajda FP, Applebaum BI, Price JC, et al. Hyperostotic esthesioneuroblastoma: CT and MR findings. *J Comput Assist Tomogr* 1988;12:52-56
8. Utsunomiya M, Ishii C, Miura S, Tada S, Kikuchi Y, Yamaguchi H. [A case of olfactory neuroblastoma with exuberant hyperostosis]. *Rinsho Hoshasen* 1989;34:1019-1022
9. Schuster JJ, Phillips CD, Levine PA. MR of esthesioneuroblastoma (olfactory neuroblastoma) and appearance after craniofacial resection. *AJNR Am J Neuroradiol* 1994;15:1169-1177
10. Iio M, Homma A, Furuta Y, Fukuda S. [Magnetic resonance imaging of olfactory neuroblastoma]. *Nihon Jibiinkoka Gakkai Kaiho* 2006;109:142-148
11. Pickuth D, Heywang-Köbrunner SH, Spielmann RP. Computed tomography and magnetic resonance imaging features of olfactory neuroblastoma: an analysis of 22 cases. *Clin Otolaryngol Allied Sci* 1999;24:457-461
12. Hurst RW, Erickson S, Cail WS, Newman SA, Levine PA, Burke J, et al. Computed tomographic features of esthesioneuroblastoma. *Neuroradiology* 1989;31:253-257
13. Vanhoenacker P, Hermans R, Sneyers W, Vanderperre H, Clarysse J, Loncke R, et al. Atypical aesthesioneuroblastoma: CT and MRI findings. *Neuroradiology* 1993;35:466-467
14. Tseng J, Michel MA, Loehrl TA. Peripheral cysts: a distinguishing feature of esthesioneuroblastoma with intracranial extension. *Ear Nose Throat J* 2009;88:E14
15. Som PM, Lidov M, Brandwein M, Catalano P, Biller HF. Sinonasal esthesioneuroblastoma with intracranial extension: marginal tumor cysts as a diagnostic MR finding. *AJNR Am J Neuroradiol* 1994;15:1259-1262
16. Zafereo ME, Fakhri S, Prayson R, Batra PS, Lee J, Lanza DC, et al. Esthesioneuroblastoma: 25-year experience at a single institution. *Otolaryngol Head Neck Surg* 2008;138:452-458
17. Schiro BJ, Escott EJ, McHugh JB, Carrau RL. Bone invasion by an esthesioneuroblastoma mimicking fibrous dysplasia. *Eur J Radiol (extra)* 2008;65:69-72
18. Bikmaz K, Mrak R, Al-Mefty O. Management of bone-invasive, hyperostotic sphenoid wing meningiomas. *J Neurosurg* 2007;107:905-912
19. Tehranzadeh J, Fung Y, Donohue M, Anavim A, Pribram HW. Computed tomography of Paget disease of the skull versus fibrous dysplasia. *Skeletal Radiol* 1998;27:664-672